IEEE Access
Multidisciplinary | Rapid Review | Open Access Journal

Received November 30, 2016, accepted December 23, 2016, date of publication January 2, 2017, date of current version January 27, 2017.

Digital Object Identifier 10.1109/ACCESS.2016.2646338

CPW Fed UWB Antenna by EBGs With Wide Rectangular Notched-Band

LIN PENG[1,2], (Member, IEEE), BAO-JIAN WEN[1], XIAO-FENG LI[1], XING JIANG[1,2], AND SI-MIN LI[1]

[1]Guangxi Key Laboratory of Wireless Wideband Communication and Signal Processing, Guilin University of Electronic Technology, Guilin 541004, China
[2]Key Laboratory of Microwave and Optical Wave-applied Technology, Guilin University of Electronic Technology, Guilin 541004, China

Corresponding author: L. Peng (penglin528@hotmail.com)

This work was supported in part by the National Natural Science Foundation of China under Grant 61661011, Grant 61401110, and Grant 61371056, in part by the Natural Science Foundation of Guangxi under Grant 2015GXNSFBA139244, and in part by the Guangxi Key Laboratory of Wireless Wideband Communication and Signal Processing under Grant GXKL06160109.

ABSTRACT Ultra-wideband (UWB) antennas with wide rectangular notched-band are proposed in this paper. The rectangular notched-band design is realized by placing dual mushroom-type electromagnetic-bandgap (EBG) structures on the CPW feeding line. The patches of the EBGs are laid on the back size of the substrate and dead against the CPW feeding line. Shorting pins are utilized to connect the patch and the feeding line. Then, the CPW feeding line operates as ground plane for the EBGs. By tuning the two resonant frequencies of the EBG structures and making them merge with each other, a rectangular notchedband is achieved. Research also found that design methodology has the ability to tune the width and the frequency of the rectangular notched-band by adjusting the EBG parameters. Then, three cases of rectangular notchedband designs to reject the wireless local-area network (WLAN, 5.150–5.825 GHz) interference band and the *X*-band downlink satellite communication band (660 MHz, 7.10–7.76 GHz) were designed by using different EBG parameters. The design methodology can also be utilized to design rectangular notchedband for other interference bands efficiently.

INDEX TERMS Rectangular notched-band, EBG, CPW line, UWB antennas.

I. INTRODUCTION

The prospective marketing for the short-range high-speed indoor data communications had accelerated the development of ultra-wideband (UWB) technologies [1]–[3]. However, the limited spectrum resource makes the UWB systems difficult to avoid interference from nearby narrowband systems. For example, the wireless local-area network (WLAN, 5.150-5.825 GHz) and the X-band downlink satellite communication band (7.10-7.76 GHz) occupy frequencies in the 2002 US-FCC released UWB band (3.1-10.6 GHz band) [4], [5].

One efficient and economical way to solve this problem is to reject the interferences at the front-end of an UWB communication system. Therefore, UWB antennas with certain frequency notched-bands make great significance. And, lots of endeavors have been dedicated to the design of UWB band-notched antennas [4]–[12]. In these researches, several approaches were proposed for notched-band design, such as etching slots on the patch/ground plane [4]–[7], coupling parasitic elements to the radiator [8], [9], using the overlap areas of split rings [10], embedding resonant cell in the microstrip line [11], and using Electromagnetic-bandgap (EBG) structure [12].

Highly-efficient notched-band design can be achieved by these techniques. However, the techniques of etching slots and coupling parasitic elements may have big impact on the current distributions of the pass-band frequencies, and the pass-band radiation patterns may be affected. Moreover, the above referred antennas have a common drawback that the notched-bands present spiculate curves. The spiculate notched-band may cripple the anti-interference function as the interferential sources occupy a definite band, such as 675 MHz for WLAN band and 660 MHz for X-band downlink satellite communication band. In [13], two spiculate notches were obtained to stop the 5.2 and 5.8 GHz bands without filtering the bandwidth in between them. However, the designing is not suitable for the rejection of a wide interference band, such as the X-band downlink satellite communication band (660 MHz).

In [14] and [15], rectangular notched-bands were obtained for UWB antennas. In [14], quarter-wavelength slits etched on the ground and half-wavelength stubs coupled to the microstrip were utilized to achieve rectangular notched-bands. In [15], several dual-split-ring-resonators were coupled to the CPW line to generate rectangular notched-band. However, the rectangular notched-band designs of [14] and [15] have complicated structures, and the complicated structures might be obstacles for high-efficiency designs. Besides, there are only a few researches on rectangular notched-band designs. Therefore, UWB antennas with rectangular notched-bands are urgently needed. And, a high-efficiency notched-band design method that capable of adjusting the notched-band frequency and width to adapt to different interference bands is preferable. The research of this paper is dedicated to develop such a method.

In this paper, a method to design rectangular notched-band for CPW fed UWB antenna is proposed. By utilizing two EBG structures with adjacent resonant frequencies in the CPW feeding line, a rectangular wide notched-band was realized. The operating mechanism and design methodology of the antennas are investigated. Research found that the notched-band frequency and width can be tuned by adjusting the EBG parameters. Two reference antennas, an UWB antenna and a spiculate notched-band UWB antenna, were designed for comparison. Three UWB antenna cases with rectangular notched-band were proposed. Good rectangular notched-band results were obtained. Research also found the EBG structures have little effect on the pass-band radiation patterns.

II. REFERENCES ANTENNAS

To highlight the rectangular notched-band characteristics of the proposed design, a CPW-fed UWB antenna and a CPW-fed UWB antenna with spiculate notch were designed as reference antennas. As demonstrated in Fig. 1 (a) and (b), the antennas are denoted as antenna 1 and antenna 2, respectively. Similar to [7], the antenna 1 has an elliptical radiator (with radius of $r_x = 13$ mm and $r_y = 9.5$ mm), however, the radiator of this design is fed by a CPW line with 50 Ω characteristic impedance ($W_f = 3.5$ mm and $g = 0.2$ mm) as shown in Fig. 1 (a). The antenna 1 was printed on a substrate with length $L_0 = 50$ mm, width $W_0 = 48$ mm, thickness $h = 1$ mm and relative permittivity $\varepsilon_r = 2.65$. The length of the ground plane is $L_1 = 30$ mm, and the gap between elliptical radiator and the ground plane is $d_0 = 0.1$ mm. Note that, when band-notched design (EBGs) is applied to the antenna 1, there is no returning work required for the previously determined dimensions.

As shown in Fig. 1 (b), the antenna 2 is designed by implanting an EBG structure to the CPW feeding line of the antenna 1. As shown in the figure, the EBG patch with width $a_1 = 3.5$ mm and length $b_1 = 7.7$ mm was placed on the back size of the substrate and it is dead against the CPW feeding line. The shorting pin with diameter of $D = 0.6$ mm connects the upper edge of the EBG patch and the CPW feeding line.

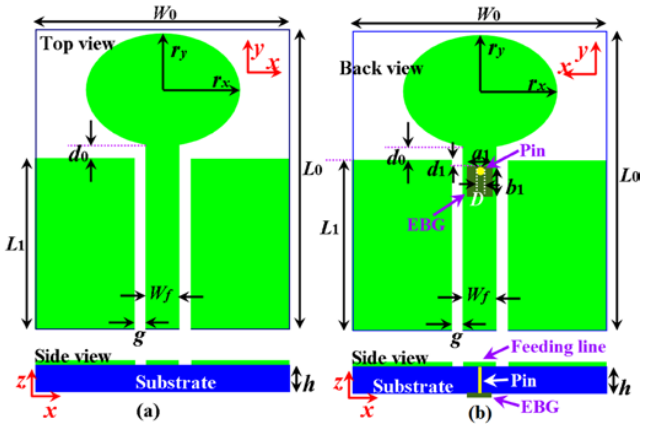

FIGURE 1. Schematic view of the reference antennas. (a) the antenna 1, and (b) the antenna 2.

Thus, in response to the EBG structure, the CPW feeding line takes the role of a ground plane. The distance between the upper edge of the ground plane and the EBG is $d_1 = 1$ mm. Though the resonant (notch) frequency is mainly determined by the EBG parameters, the distance d_1 still has effect on the notch width and depth (the simulated results are not shown here for simplicity).

The results (S_{11} and Z_{11}) of the antenna 1 and the antenna 2 were plotted in Fig. 2 (a) and (b), respectively. As depicted in Fig. 2 (a), the antenna 1 displays smooth Z_{11} curves with nearly 50 Ω Re(Z_{11}) and nearly 0 Ω Im(Z_{11}) for the whole UWB band. Then, the antenna 1 obtains good impedance matching with the simulated band ($S_{11} < -10$ dB) ranges from 2.74 GHz to beyond 11 GHz and the measured band ranges from 2.66 GHz to beyond 10 GHz. As shown in Fig. 2 (b), the Z_{11} behaviors of the antenna 2 are similar to the antenna 1 except for the frequencies around 5.54 GHz. For the frequencies around 5.54 GHz, the Re(Z_{11}) rise to a very large value suddenly and the Im(Z_{11}) also has sudden changing, then, the 5.54 GHz is the resonant frequency of the EBG structure. As the resonance of the EBG structure makes singular input impedance, a peak notch (notch frequency) can be observed at 5.54 GHz and a notched-band with $S_{11} > -10$ dB can also be obtained around the notch frequency. As shown in Fig. 2 (b), both the simulated and measured S_{11} curve of the antenna 2 display a notched-band around the resonance. The simulated notched-band is 4.49-6.08 GHz ($S_{11} > -10$ dB) with a notch frequency of 5.54 GHz, and the measured notched-band is 4.64-6.22 GHz with a notch frequency of 5.68 GHz. Unfortunately, the notched-band width of the antenna 2 is 1590/1580 MHz for simulation/measurement, and the notched-band leads to useful frequencies rejection. Moreover, the notched band shows spiculate shape and debased frequency-reject function for the fringe frequencies near 5.15 GHz and 5.825 GHz as the simulated/measured S_{11} values for 5.15 GHz and 5.825 GHz are about −4.2/−5.58 dB and −4.5/−3.55 dB, respectively.

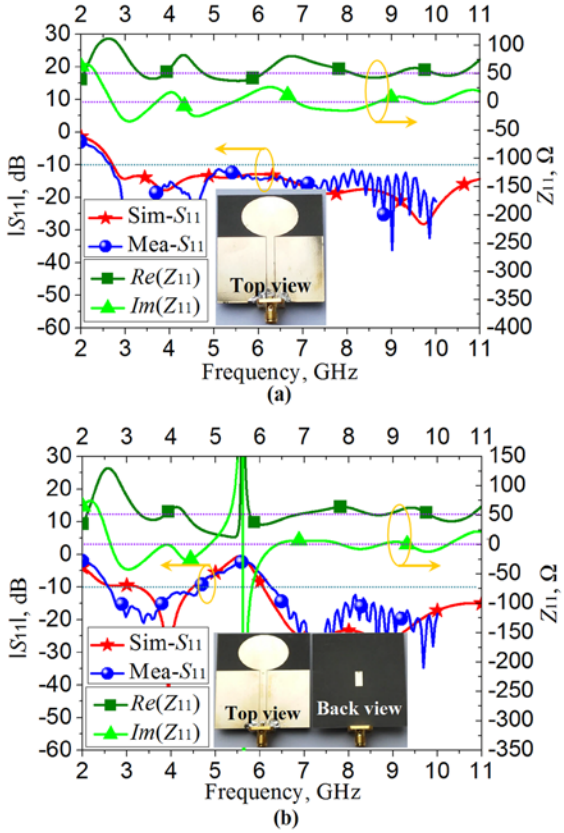

FIGURE 2. S_{11} and Z_{11} of the reference antennas. (a) the antenna 1 and (b) the antenna 2.

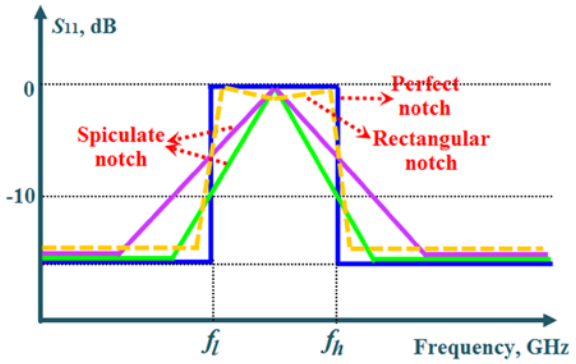

FIGURE 3. Notched-bands.

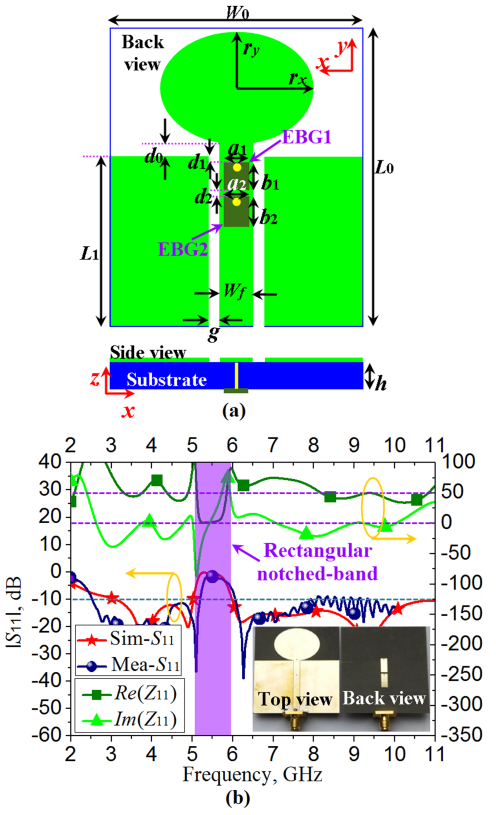

FIGURE 4. The antenna 3. (a) schematic view, (b) S_{11} and Z_{11} of the case 1.

III. CPW FED RECTANGULAR NOTCHED-BAND UWB ANTENNA DESIGN

A. RECTANGULAR NOTCHED-BAND UWB ANTENNA DESIGN AND ANALYSIS

The drawbacks of spiculate notched-band require perfect notch to perfectly stop interference frequencies from f_l to f_h and avoid useful frequencies rejection as depicted in Fig. 3. Easily come to the conclusion that, it is hard (or impossible) to realize a perfect notch. However, as described in Fig. 3, we may achieve a rectangular notched-band by merging two or multi-resonances (notches). Inspired by the idea, a dual-EBGs notch design was proposed for the UWB antenna as shown in Fig. 4 (a). As shown in the figure, two EBG structures (named EBG1 and EBG2) were arranged in a line on the CPW feed line. The antenna is denoted as antenna 3.

Here, we give a case for the EBG parameters of the antenna 3 as $a_1 = 3.5$ mm, $b_1 = 7.9$ mm, $d_1 = -1$ mm, $a_2 = 3.5$ mm, $b_2 = 7.7$ mm, $d_2 = 1$ mm and $D = 0.6$ mm. It is denoted as case 1 of antenna 3 and two more cases of antenna 3 will be designed in the next sub-section.

The results (S_{11} and Z_{11}) of the case 1 are plotted in Fig. 4 (b). As shown in the figure, two resonances of 5.05 GHz and 5.95 GHz are inspired by the EBG1 and the EBG2, respectively. The two resonances happened at closely frequencies (900 MHz distance) and merge with each other. Then, the values of Re(Z_{11}) almost equal to zero for the frequencies between the resonances and forms a rectangular pit while violent changing occurred for the Im(Z_{11}). Therefore, for frequencies within the rectangular pit, the EBGs operate as pure-reactance-loads to the antenna. Moreover, the input impedances present sharp transformations. These characteristics indicate a sharp rectangular wide notched-band. Besides, by compared to the Z_{11} curves of the antenna 1, the EBGs have little impact on the pass-band frequencies.

The case 1 of the antenna 3 was fabricated and measured as also demonstrated in Fig. 4 (b). Reasonable good agreement between the simulated and measured S_{11} are observed.

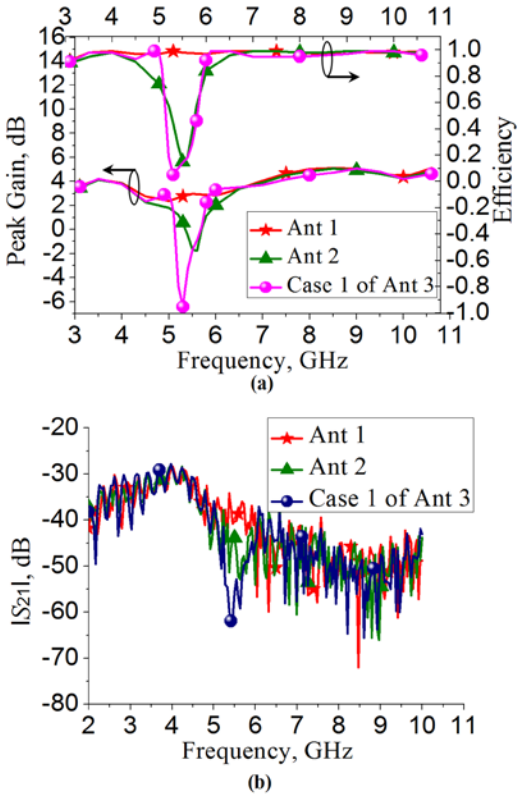

FIGURE 5. Comparison of the peak gain/ efficiency and S_{21} of the antenna 1, the antenna 2 and the antenna 3. (a) Simulated peak gain/ efficiency, and (b) measured S_{21}.

As predicted, sharp rectangular notched-bands are observed for both simulated and measured S_{11} curves. As shown in the figure, the simulated notched-band ($S_{11} > -10$ dB) ranges from 5.03 GHz to 5.98 GHz and the measured notched-band ranges from 5.19 GHz to 6.05 GHz. Then, the notched-bandwidth for simulation and measurement are 950 MHz and 860 MHz, respectively. By compared to the S_{11} curves of the antenna 2, it can be concluded that the case 1 of the antenna 3 has better interference rejection characteristic than antenna 2 and less useful frequencies injury.

To further emphasize the rectangular notched-band characteristic and the superiority of the proposed antenna 3, the simulated efficiency/peak gain and the measured transmission coefficient S_{21} of the case 1 are plotted in Fig. 5 (a) and (b), respectively. The results of the antenna 1 and the antenna 2 were also demonstrated in the figures for comparison. As shown in Fig. 5 (a), the antennas exhibit similar gain curves and efficiency curves in the pass-band with peak gain varies from 2.38-5.11 dBi and efficiency about 0.97. In the notched-band, peak gain drops from 2.38 dBi of antenna 1 to -1.73 dBi of antenna 2 and -6.45 dBi of the case 1. Meanwhile, in the notched-band, the lowest efficiencies are 0.15 and 0.05 for the antenna 2 and the case 1, respectively. Correspond to the S_{11} behavior of Fig. 2 (b), the gain/efficiency descending in the notched-band of antenna 2 is wider than the case 1, and sharp rectangular pit in the notched-band is observed for the case 1. For the case 1, the gain values of 5.15 GHz and 5.825 GHz are -1.52 dBi and 2.26 dBi, respectively. While the efficiency in the 5.15-5.825 GHz band range from 0.05 to 0.52. Fig. 5 (b) presents the measured S_{21} of the antennas. Note that, the S_{21} in this paper are measured by orientating two identical antennas face-to-face with a distance of 450 mm. As shown in the figure, transmission pits are observed for the antenna 2 and the case 1 in the stop-band, and the case 1 shows better frequency rejection characteristic.

To reveal the operating mechanism of the rectangular notched-band design, current distributions of the case 1 were displayed in Fig. 6. The current distributions of the two pass-band frequencies of 3.5 GHz and 9.5 GHz were demonstrated in Fig. 6 (a) and (b), respectively, while the current distributions of the two notch frequencies of 5.05 GHz and 5.95 GHz were plotted in Fig. 6 (c) and (d), respectively. The current distributions of the antenna 1 were also plotted in the figures for comparison. As shown in Fig. 6 (a) and (b), the current distributions of the antenna 1 and the case 1 have similar behaviors for 3.5 GHz and 9.5 GHz. Thus, the EBG structures have little effect on antenna performances for these pass-band frequencies. For 5.05 GHz and 5.95 GHz, current distribution of the antenna 1 and the case 1 are different as shown in Fig. 6 (c) and (d). As shown in the labels of Fig. 6 (c) and (d), the maximal current values of the case 1 are much larger than the antenna 1, it is because more currents are concentrated at the EBG structures for the case 1. Then, more currents of the antenna 1 pass through to the radiator and powers can be effectively radiated. While for the case 1, currents of 5.05 GHz and 5.95 GHz are concentrated at the EBG1 and the EBG2 (owing to the resonances of the EBGs), respectively, and the powers are reflected back to the port. Therefore, the two EBGs achieve a rectangular notched-band. It can be conjectured that, the two resonant frequencies can be tuned independently by adjusting their corresponding EBG parameters.

The comparisons of the radiation patterns for the antenna 1 and the case 1 were presented in Fig. 7. Fig. 7 (a), (b), (c) and (d) plot the patterns of 3.5 GHz, 5.3 GHz, 6.5 GHz and 9.5 GHz, respectively. The antennas are printed in the xy-plane, and they are y-polarized as the monopoles are in the y-direction. Therefore, the E-plane for these antennas is the yz-plane and the H-plane is the xz-plane. As shown in the figures, reasonable good agreements are observed between the simulated and measured results. The discrepancies between the simulations and the measurements are probably due to the assembling deviation of the antennas by the limitation of the measured system. However, the measured results verified the validity of the simulations. As shown in Fig. 7 (a), (c) and (d), the radiation patterns of the case 1 are very similar to their counterparts of the antenna 1 in the pass-band, even for the frequency of 6.5 GHz that is close to the notched-band. Thus, the introduction of the EBGs has little effect on the pass-band radiation patterns. For the notched-band frequency of 5.3 GHz, as exhibited in Fig. 7 (b), the EBGs make heavy impacts on the patterns of the case 1

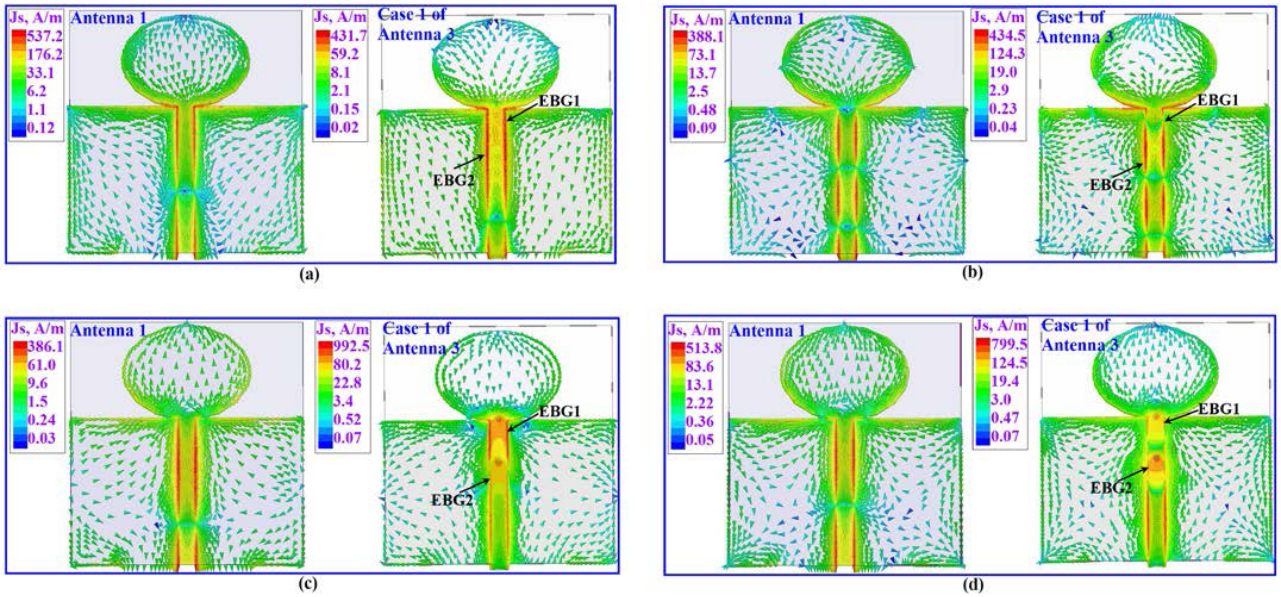

FIGURE 6. Current distributions of the case 1 of antenna 3 and the antenna 1. (a) 3.5 GHz, (b) 9.5 GHz, (c) 5.05 GHz and 5.95 GHz.

and reject power radiation. These characteristics are coincidence with the current distributions of Fig. 6. For the pass-band frequencies, the radiation patterns in the E-plane are roughly a dumbbell shape, and the patterns in the H-plane are quite omni-directional.

To further investigate the effects of the EBGs on the notched-band, two EBG parameters b_1 and b_2 were swept. Note that, when one parameter is swept, others are fixed. The parametric study results (S_{11} and Re(Z_{11})) of b_1 and b_2 were demonstrated in Fig. 8 (a) and (b), respectively. Note that, the Im(Z_{11}) curves are not exhibited here for simplicity. From the S_{11} curves in Fig. 8 (a), the -10 dB low-cutoff frequency of the rectangular notched-band drops from 5.03 GHz to 4.83 GHz and 4.59 GHz for b_1 increasing from 7.9 mm to 8.3 mm and 8.7 mm while the high-cutoff frequency is almost unchanged. The Re(Z_{11}) curves plotted in Fig. 8 (a) are accorded with the S_{11} curves as b_1 increasing extends the low-edge of the rectangular pit to lower frequency. The S_{11} and Re(Z_{11}) curves plotted in Fig. 8 (b) indicate that the b_2 mainly affects the high resonance. Therefore, with the b_2 decreased from 7.7 mm to 7.4 mm and 7.1 mm, the high-cutoff frequency increased from 5.98 GHz to 6.15 GHz and 6.51 GHz, and the rectangular pit of Re(Z_{11}) curve has similar characteristics. Therefore, the parameter b_1 and b_2 are useful parameters to adjust the width of the notched-band. Moreover, the b_1 andb_2 are also valuable parameters for notch frequency tuning.

B. MORE EXAMPLES ON RECTANGULAR NOTCHED-BAND UWB ANTENNA

From the above discussion, the antenna 3 is capable of tuning the notch frequency and the notched-band width by adjusting the EBG parameters. Therefore, two more cases of the antenna 3 were designed. One case, denoted as case 2, achieves an enhanced notched-band to fix the unsatisfactory notched-band characteristics of the case 1. The other, named as case 3, covers the X-band downlink satellite communication band (660 MHz, 7.10-7.76 GHz). The EBGs parameters for the cases are as follow:

case 2 of antenna 3: $a_1 = 3.5$ mm, $b_1 = 8.1$ mm, $d_1 = -1$ mm, $a_2 = 3.5$ mm, $b_2 = 7.4$ mm, $d_2 = 1$ mm and $D = 0.6$ mm.

case 3 of antenna 3: $a_1 = 2.8$ mm, $b_1 = 5.6$ mm, $d_1 = 0$ mm, $a_2 = 2.8$ mm, $b_2 = 5.8$ mm, $d_2 = 1.8$ mm and $D = 0.6$ mm.

The simulated and measured S_{11} curves of the case 2 and the case 3 were demonstrated in Fig. 9. The S_{11} curves of the case 1 were also plotted in the figure for comparison. Good agreements between the simulated and the measured results were obtained for both the case 1 and the case 2. As the EBG parameters of the case 2 are gained by increasing b_1 and decreasing b_2 of the case 1, the rectangular notched-band of the case 2 is wider than that of the case 1 as expected. The simulated and measured -10 dB notched-band width of the case 2 are 4.92-6.16 GHz and 5.09-6.13 GHz, respectively. Thus, the simulated/measured notched-band of the case 2 is 290/180 MHz wider than the case 1. The simulated/measured S_{11} values of the case 2 at the fringe frequencies of 5.15 GHz and 5.825 GHz are $-0.64/-3.46$ dB and $-1.33/-2.09$ dB, respectively, and they are also better than the case 1. The simulated and measured results of the case 3 are in reasonable good agreement. A rectangular notched-band is successfully achieved in the X-band downlink satellite communication band. The simulated and measured -10 dB notched-band are 7.04-7.85 GHz and 7.25-8.11 GHz, respectively.

The simulated efficiency/peak gain and the measured S_{21} of the three cases of the antenna 3 were plotted in Fig. 10

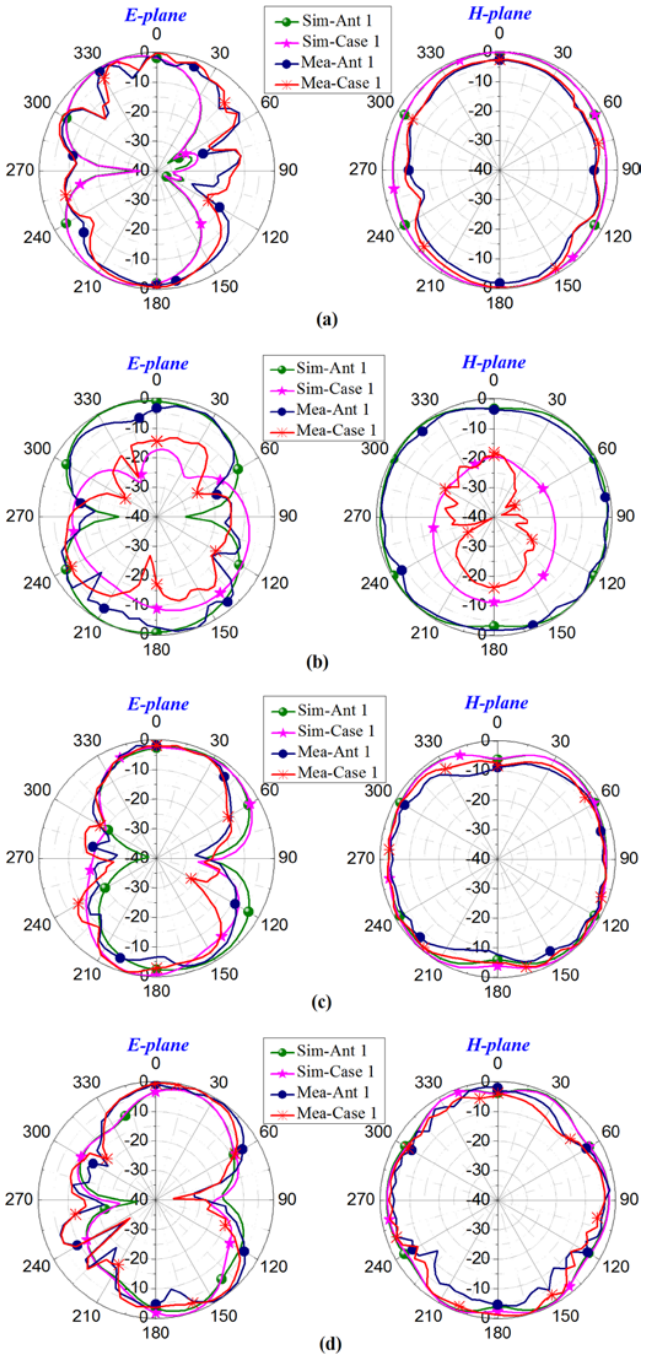

FIGURE 7. Radiation pattern comparison for the antenna 1 and the case 1 of antenna 3. (a) 3.5 GHz, (b) 5.3 GHz, (c) 6.5 GHz, and (d) 9.5 GHz.

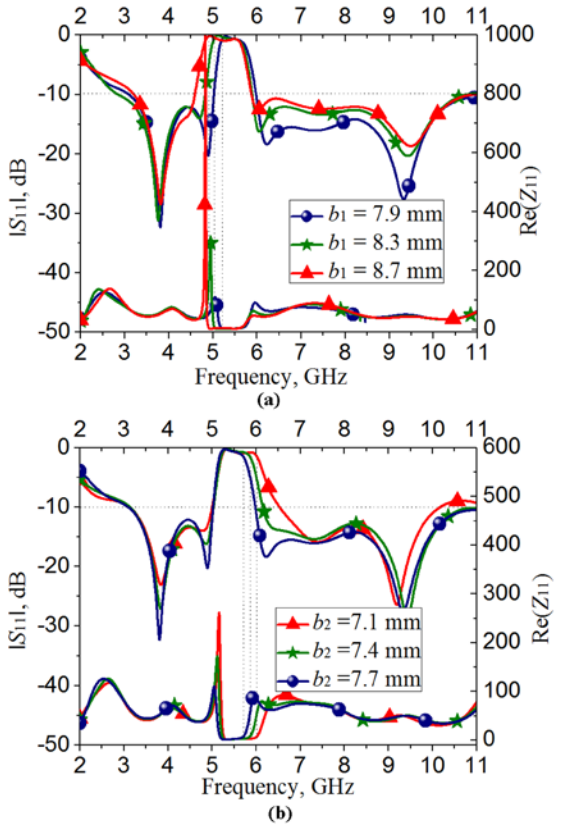

FIGURE 8. Parametric study. (a) b_1, and (b) b_2.

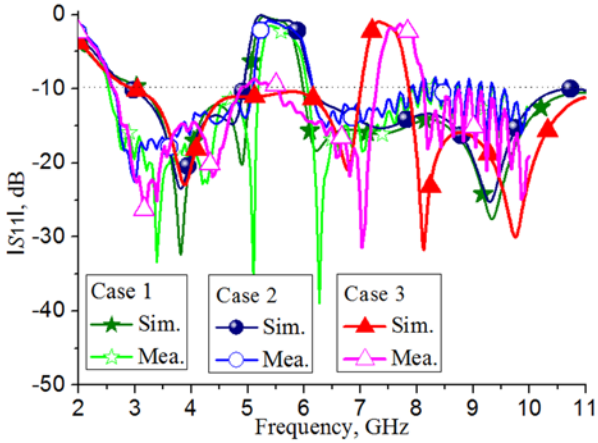

FIGURE 9. Comparison for S_{11} of the case 1, 2 and 3 of antenna 3.

for comparison. Fig. 10 (a) and (b) present the efficiency/peak gain and the S_{21}, respectively. For both the efficiency/peak gain and the S_{21}, rectangular gaps were observed at the WLAN band for the case 1 and the case 2, and rectangular gaps are realized at the X-band downlink satellite communication band for the case 3. The three cases present similar behavior at the pass-band. The peak gain values of the case 2 at 5.15 GHz and 5.825 GHz are −5.7 dBi and −0.42 dBi, respectively. Besides, the gain values of the 5.15-5.825 GHz band range from −0.42 to −9.76 dBi for the case 2, while it is 2.26 to −6.45 dBi for the case 1 in the same interference band. While the efficiency in the 5.15-5.825 GHz band range from 0.03 to 0.22 for the case 2. The measured S_{21} curve of the case 2 exhibits a 20-40 dB frequency rejection improvement in the notched-band, and the case 2 also exhibits better frequency rejection characteristic than the case 1. The transmission forbidden band of the case 2 is about 5.14-5.91 GHz. The case 3 realizes about 4 dB in gain reduction and large efficiency reduction at the X-band, and the measured S_{21} rectangular gap achieves 15 dB frequency rejection improving.

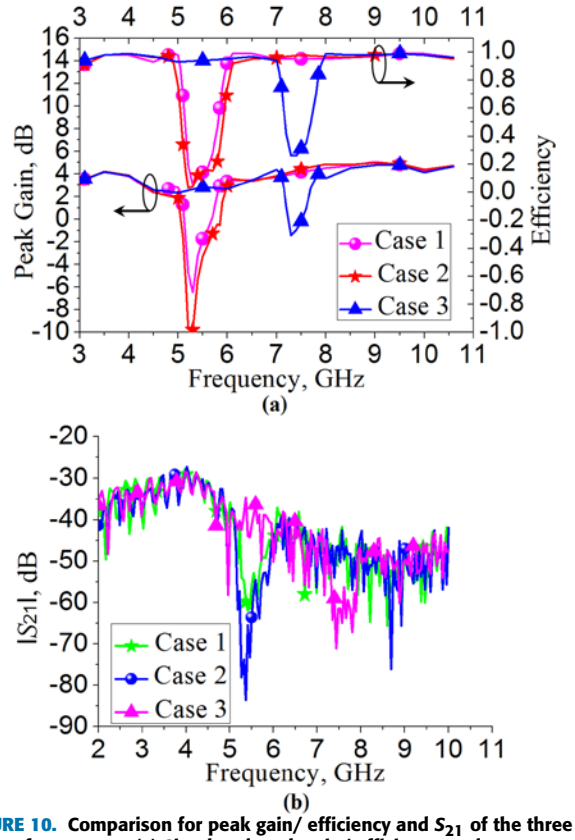

FIGURE 10. **Comparison for peak gain/ efficiency and S_{21} of the three cases of antenna 3. (a) Simulated peak gain/ efficiency, and (b) Measured S_{21}.**

In keeping with the main focus of notched-band design, the radiation patterns of the case 2 and the case 3 are not presented here for simplicity.

IV. CONCLUSION

Novel methodology for rectangular notched-band design is proposed. The method utilizes two EBG structures with close resonances in the feeding line. Then, the rectangular notched-band can be controlled by the EBGs. Therefore, the method can be easily adjusted to different interference bands. Three prototypes with rectangular notched-band were design and measured. The antennas are good candidates for UWB systems.

REFERENCES

[1] T. Ali, P. Siddiqua, and M. A. Matin, "Performance evaluation of different modulation schemes for ultra wide band systems," *J. Elect. Eng.*, vol. 65, no. 3, pp. 184–188, 2014.

[2] W. Wiesbeck, G. Adamiuk, and C. Sturm, "Basic properties and design principles of UWB antennas," *Proc. IEEE*, vol. 97, no. 2, pp. 372–385, Feb. 2009.

[3] A. M. Abbosh and M. E. Bialkowski, "Design of ultrawideband planar monopole antennas of circular and elliptical shape," *IEEE Trans. Antennas Propag.*, vol. 56, no. 1, pp. 17–23, Jan. 2008.

[4] M. M. Fakharian, P. Rezaei, and A. Azadi, "A planar UWB bat-shaped monopole antenna with dual band-notched for WiMAX/WLAN/DSRC," *Wireless Pers. Commun.*, vol. 81, no. 2, pp. 881–891, 2014.

[5] P. S. Bakariya, S. Dwari, and M. Sarkar, "A triple band notch compact UWB printed monopole antenna," *Wireless Pers. Commun.*, vol. 82, no. 2, pp. 1095–1106, Feb. 2015.

[6] X. L. Yang, F. L. Kong, and Y. Wang, "A smile face monopole antenna with quadruple band-notched characteristics," *Frequenz*, vol. 69, nos. 5–6, pp. 185–191, 2015.

[7] K. Bahadori and Y. Rahmat-Samii, "A miniaturized elliptic-card UWB antenna with WLAN band rejection for wireless communications," *IEEE Trans. Antennas Propag.*, vol. 55, no. 11, pp. 3326–3332, Nov. 2007.

[8] M. Abedian, S. K. A. Rahim, S. Danesh, S. Hakimi, L. Y. Cheong, and M. H. Jamaluddin, "Novel design of compact UWB dielectric resonator antenna with dual-band-rejection characteristics for WiMAX/WLAN bands," *IEEE Antennas Wireless Propag. Lett.*, vol. 14, pp. 245–248, 2015.

[9] M. Ojaroudi and N. Ojaroudi, "Ultra-wideband small rectangular slot antenna with variable band-stop function," *IEEE Trans. Antennas Propag.*, vol. 62, no. 1, pp. 490–494, Jan. 2014.

[10] L. Peng, J. Y. Xie, X. Jiang, and S. M. Li, "Investigation on ring/split-ring loaded bow-tie antenna for compactness and notched-band," *Frequenz*, vol. 70, nos. 3–4, pp. 89–99, 2016.

[11] S. W. Qu, J. L. Li, and Q. Xue, "A band-notched ultrawideband printed monopole antenna," *IEEE Antennas Wireless Propag. Lett.*, vol. 5, pp. 495–498, 2006.

[12] L. Peng and C. L. Ruan, "UWB band-notched monopole antenna design using electromagnetic bandgap structures," *IEEE Trans. Microw. Theory Techn.*, vol. 59, no. 4, pp. 1074–1081, Apr. 2011.

[13] A. A. Gheethan and D. E. Anagnostou, "Dual band-reject UWB antenna with sharp rejection of narrow and closely-spaced bands," *IEEE Trans. Antennas Propag.*, vol. 60, no. 4, pp. 2071–2076, Apr. 2012.

[14] W. A. Li, Z. H. Tu, Q. X. Chu, and X. H. Wu, "Differential stepped-slot UWB antenna with common-mode suppression and dual sharp-selectivity notched bands," *IEEE Antennas Wireless Propag. Lett.*, vol. 15, pp. 1120–1123, Sep. 2016.

[15] J. Y. Siddiqui, C. Saha, and Y. M. M. Antar, "Compact dual-SRR-loaded UWB monopole antenna with dual frequency and wideband notch characteristics," *IEEE Antennas Wireless Propag. Lett.*, vol. 14, pp. 100–103, 2015.

LIN PENG (M'16) was born in Guangxi, China, in 1981. He received the B.E. degree in science and technology of electronic information, and the master's and Ph.D. degrees in radio physics from the University of Electronic Science and Technology of China, Chengdu, China, in 2005, 2008, and 2013, respectively.

From 2011 to 2013, he was sponsored by the China Scholarship Council to study from the University of Houston as joint Ph.D. student. Since 2013, he has been with the Guilin University of Electronic Technology, and he became an Associate Professor from 2016. He has published over 20 papers as first and corresponding author. He is also co-author with over 20 papers. His research interests include antenna/filter design (For example: communication antennas, zeroth-order resonator antenna, circular-polarized antenna, ultrawide band antenna, microstrip antenna, and WLAN antenna), electromagnetic bandgap structure design and its application in antenna, composite right/left-handed transmission line and its applications, and conformal antenna array.

In recent years, he is sponsored by several funds, such as Fundamental Research Funds for the Central Universities, the National Natural Science Foundation of China, the Natural Science Foundation of Guangxi, the Program for Innovative Research Team of Guilin University of Electronic Technology, and Guangxi Wireless Broadband Communication and Signal Processing Key Laboratory. He serve as an Reviewer of the IEEE Transaction on Microwave Theory and Techniques, the IEEE Microwave and Wireless Components Letters, *Wireless Personal Communications*, *Progress in Electromagnetics Research*, *IET Microwave, Antennas & Propagation*, and *Journal of Electromagnetic Waves and Applications*.

BAO-JIAN WEN was born in Guangxi, China, in 1989. He received the B.E. degree in communication engineering from the Chengdu University of Information Technology, Sichuan, China, in 2014. He is currently pursuing the master's degree with the Guilin University of Electronic Technology. His research interests include antennas and metamaterials.

XIAO-FENG LI was born in Shaanxi, China. He received the B.E. degree from Northwest Normal University, Lanzhou, China, in 1993, and the master's degree from Lanzhou University in 2006. He is currently a Lecturer with the Guilin University of Electronic Technology. His research interests include antennas and electromagnetic measurements.

XING JIANG received the master's degree in electromagnetic field and microwave technology from the Beijing Institute of Technology, in 1986. Since 2000, she has been with the Guilin University of Electronic Technology as a Professor. She has published over 30 papers. Her research interests include smart communication system design, conformal antenna array, and bio-electromagnetics. She also sponsored by the National Natural Science Foundation of China and the Natural Science Foundation of Guangxi. She is a Senior Member of China Communications Society, a member of the Chinese Institute of Electronics.

SI-MIN LI received the B.S. degree in wireless communication engineering from the Nanjing University of Posts and Telecommunications, Jiangsu, China, in 1984, and the M.S. and Ph.D. degrees in electronics engineering from the University of Electronic Science and Technology of China, Chengdu, China, in 1989 and 2007, respectively.

From 1984 to 1986, he was an Engineer Assistant with Optical Communication Department, Wuhan Post-Telecommunications Science and Research Institute. From 1989 to 2005, he was a Lecturer, Assistant Professor, and Professor with the School of Information and Communication, Guilin University of Electronic Technology. He is currently a President and a Professor with the Guangxi University of Science and Technology, Liuzhou, China. His current research interests include the design of electrically small antennas, antenna arrays for high-frequency communication systems, and wireless sensor networks.